Estimating the macroscopic capillary length from Beerkan infiltration experiments and its impact on saturated soil hydraulic conductivity predictions

Original

Estimating the macroscopic capillary length from Beerkan infiltration experiments and its impact on saturated soil hydraulic conductivity predictions / Di Prima, S.; Stewart, R. D.; Castellini, M.; Bagarello, V.; Abou Najm, M. R.; Pirastru, M.; Giadrossich, F.; Iovino, M.; Angulo-Jaramillo, R.; Lassabatere, L.. - In: JOURNAL OF HYDROLOGY. - ISSN 0022-1694. - 589:(2020), p. 125159. [10.1016/j.jhydrol.2020.125159]

Published
DOI:10.1016/j.jhydrol.2020.125159

Estimating the macroscopic capillary length from Beerkan infiltration experiments and its impact on saturated soil hydraulic conductivity predictions

Simone Di Prima [a,b*], Ryan D. Stewart [c], Mirko Castellini [d], Vincenzo Bagarello [e], Majdi R. Abou Najm [f], Mario Pirastru [a], Filippo Giadrossich [a], Massimo Iovino [e], Rafael Angulo-Jaramillo [b] and Laurent Lassabatere [b]

[a] Department of Agricultural Sciences, University of Sassari, Viale Italia, 39, 07100 Sassari, Italy.
[b] Université de Lyon; UMR5023 Ecologie des Hydrosystèmes Naturels et Anthropisés, CNRS, ENTPE, Université Lyon 1, Vaulx-en-Velin, France.
[c] School of Plant and Environmental Sciences, Virginia Polytechnic Institute and State University, Blacksburg, VA, United State.
[d] Council for Agricultural Research and Economics-Agriculture and Environment Research Center (CREA-AA), Via Celso Ulpiani 5, 70125 Bari, Italy.
[e] Department of Agricultural, Food and Forest Sciences, University of Palermo, Palermo, Italy.
[f] Department of Land, Air and Water Resources, University of California, Davis, CA 95616, United States.
* Corresponding Author. E-mail: sdiprima@uniss.it

Abstract

The macroscopic capillary length, λ_c, is a fundamental soil parameter expressing the relative importance of the capillary over gravity forces during water movement in unsaturated soil. In this investigation, we propose a simple field method for estimating λ_c using only a single-ring infiltration experiment of the Beerkan type and measurements of initial and saturated soil water contents. We assumed that the intercept of the linear regression fitted to the steady-state portion of the experimental infiltration curve could be used as a reliable predictor of λ_c. This hypothesis was validated by assessing the proposed calculation approach using both analytical and field data. The analytical validation demonstrated that the proposed method was able to provide reliable λ_c estimates over a wide range of soil textural characteristics and initial soil water contents. The field testing was performed on a large database including 433 Beerkan infiltration experiments, with the 99% of the experiments yielding realistic λ_c values. The generated λ_c values were then used in conjunction with four different methods for estimating saturated soil hydraulic conductivity, K_s. Estimated K_s values were close to those generated by a reference method, with relative error < 25% in nearly all cases. By comparison, assuming constant or soil-dependent λ_c values caused relative errors in K_s of up to 600%. Altogether, the proposed method constitutes an easy solution for estimating λ_c, which can improve our ability to estimate K_s in the field.

Keywords: infiltration, macroscopic capillary length, Beerkan, ring infiltrometer, hydraulic conductivity.

Highlights

- The macroscopic capillary length (λ_c) is a key hydraulic parameter.
- We propose a simple field method to estimate λ_c from steady-state infiltration.
- We assessed the proposed calculation approach using both analytical and field data (n = 433).
- The proposed method can improve our ability to estimate hydraulic conductivity in the field.

1. Introduction

The macroscopic capillary length, λ_c (L), was first described by Bouwer (1964) and expresses the relative importance of capillary over gravity forces during water movement in unsaturated soil (Raats, 1976). More specifically, low λ_c values (e.g., $0 < \lambda_c \leq 10$ mm) indicate a dominance of gravity over capillarity, and are typically found in coarse-textured or highly structured porous media (Reynolds et al., 2002). Alternately, high λ_c values (i.e., > 1000 mm) indicate dominance of capillarity over gravity, as found in many fine-textured or poorly structured porous media (**Table 1**). λ_c can also be used to estimate the macroscopic pore radius (i.e., the average radius of the pores that are active in flow) via the Young-Laplace equation (Kutilek and Nielsen, 1994), as suggested by Roulier et al. (2002). Because it indicates soil capillarity, λ_c is included in many infiltrometer methods for calculating K_s (e.g., Bagarello et al., 2017, 2014d, 2004; Elrick and Reynolds, 1992; Nimmo et al., 2009; Reynolds and Elrick, 1990; Stewart and Abou Najm, 2018a; Wu et al., 1999). It is thus important to accurately constrain λ_c under field conditions.

Previously developed methods to estimate λ_c have all presented some limitations. For instance, the two-ponding depths method by Reynolds and Elrick (1990) requires measuring steady state flow rates under two distinct water ponding conditions, thus inducing considerable effort and experimental complexity. Bagarello et al. (2013) proposed empirical equations to estimate λ_c;

however, those results were site specific and therefore lacked generality. In addition, those authors used the cumulative linearization method (Smiles and Knight, 1976), which can fail in the presence of layered media, entrapped air, and vertical soil water content gradients (Vandervaere et al., 2000). Other methods are based on the analysis of transient state data, as for the case of the Method 1 by Wu et al. (1999) and Approach 2 by Stewart and Abou Najm (2018a). However, these approaches require accurate characterization of the transient state, which can be challenging under specific field conditions such as highly permeable, slightly sorptive and water-repellent soils (Di Prima et al., 2019). Therefore, alternative methods for estimating λ_c from simple and replicable infiltration experiments have the potential to substantially reduce the amount of work necessary to accurately estimate soil hydraulic properties.

The first objective of this investigation was to validate a simple field method to estimate λ_c that requires only a single-ring infiltration experiment taken to steady-state conditions (Lassabatere et al., 2006) and estimates for initial and saturated soil water contents. To meet this objective, we first developed the theoretical analysis for the estimation of λ_c from a single Beerkan run. We then validated the proposed method using analytically generated data, involving soils with different texture and initial water contents, and an empirical infiltration database that included data from 433 field measurements collected during previous investigations. The second objective was to evaluate how λ_c values generated by our approach affected predictions of K_s from infiltration experiments. Here we used four different models to estimate K_s from steady-state infiltration, and then compared those results with both reference values and with those estimated using constant and soil-dependent λ_c values.

2. Theory

For water infiltrating into an unsaturated soil from a constant head source, the soil matric flux potential, ϕ_m (L^2 T^{-1}), is defined as (Gardner, 1958):

$$\phi_m = \int_{h_i}^{h_0} K(h)dh \qquad h_i \leq h \leq h_0 \tag{1a}$$

where K (L T^{-1}) is hydraulic conductivity and h (L) is water pressure head, with an initial value h_i (L) and a source pressure head h_0 (L). Eq. (1a) simplifies to Eq. (1b) when water infiltrates from a ponded source:

$$\phi_m = \int_{h_i}^{0} K(h)dh \qquad h_i \leq h \leq 0 \tag{1b}$$

The macroscopic capillary length, λ_c (L), is defined as (Philip, 1985; Smith et al., 2002):

$$\lambda_c = \frac{\phi_m}{\Delta K} \tag{2}$$

where ΔK represents the difference between the saturated soil hydraulic conductivity, K_s (L T^{-1}), and the initial soil hydraulic conductivity, K_i (L T^{-1}), i.e., $\Delta K = K_s - K_i$.

According to White and Sully (1987), Eq. (2) can be rewritten as:

$$\lambda_c = \frac{b\, S^2}{\Delta\theta\, \Delta K} \tag{3}$$

where b is a dimensionless constant dependent on the shape of the soil water diffusivity function, S (L T$^{-0.5}$) is the soil sorptivity (Philip, 1957), $\Delta\theta$ stands for the difference between the saturated, θ_s (L^3 L^{-3}), and initial, θ_i (L^3 L^{-3}), volumetric soil water contents, i.e., $\Delta\theta = \theta_s - \theta_i$. For field soils, b is commonly set equal to 0.55 even though it can theoretically vary from 1/2 to $\pi/4$ (White and Sully, 1987). K_i is often assumed negligible, such that $\Delta K = K_s$ (White and Sully, 1992).

Estimating λ_c with Eq. (3) requires prior determination of sorptivity and hydraulic conductivity. These quantities can be estimated thanks to water infiltration experiments and fitting to the quasi-exact implicit (QEI) model developed by Haverkamp et al. (1994) or its related approximate expansions (see Lassabatere et al., 2009 for more details). Haverkamp et al. (1994) proposed the following approximate expansion for the description of the steady-state for three-dimensional (3D) water infiltration from a disc source while maintaining a zero water pressure head at the soil surface:

$$I_{3D}^{+\infty}(t) = \left(K_s + \frac{\gamma S^2}{r\Delta\theta}\right) t + \frac{S^2}{2(1-\beta)\Delta K} ln\left(\frac{1}{\beta}\right) \tag{4}$$

where r (L) is the radius of the source, and γ and β are two infiltration constants, often fixed at $\gamma = 0.75$ and $\beta = 0.6$ (Haverkamp et al., 1994). Eq. (4) was later extended to include infiltration experiments from cylindrical sources with a slightly ponded water source (Ross et al., 1996) with negligible effect on results.

Eq. (4) is a linear equation of the form:

$$I_{3D}^{+\infty}(t) = i_s\, t + b_s \tag{5}$$

with b_s (L) and i_s (L T^{-1}) defined as functions of hydraulic conductivity and sorptivity as follows:

$$i_s = K_s + \frac{\gamma S^2}{r\Delta\theta} \tag{6a}$$

$$b_s = \frac{S^2}{2(1-\beta)\Delta K} ln\left(\frac{1}{\beta}\right) \tag{6b}$$

In this study, we use Eq. (6b) to quantify the ratio between sorptivity and the difference in hydraulic conductivity, as previously suggested by Castellini et al. (2018):

$$\frac{S^2}{\Delta K} = \frac{b_s}{C} \tag{7a}$$

$$C = \frac{1}{2(1-\beta)} ln\left(\frac{1}{\beta}\right) \tag{7b}$$

Eqs. (3) and (7) can be combined to explicitly solve for λ_c:

$$\lambda_c = \frac{b\, S^2}{\Delta\theta\, \Delta K} = \frac{b}{\Delta\theta} \frac{b_s}{C} \tag{8a}$$

$$\lambda_c = \frac{b}{\frac{1}{2(1-\beta)} ln\left(\frac{1}{\beta}\right)} \frac{b_s}{\Delta\theta} \tag{8b}$$

Under the common assumptions that $b = 0.55$ and $\beta = 0.6$, Eq. (8b) can be simplified as follows:

$$\lambda_c = 0.861 \frac{b_s}{\Delta\theta} \tag{9}$$

Eq. (9) constitutes a considerable simplification, as λ_c can now be estimated by only using the steady-state infiltration data (to determine b_s) and a measurement of the initial and saturated soil water contents, θ_i and θ_s. Indeed, b_s is calculated as the intercept of the linear regression fitted to the steady-state portion of the experimental infiltration curve (Eq. 5), so b_s calculation does not require the use of Eq. (6b). Note that the simplified proposed method combines equations related to two approaches with distinct, but not necessarily incompatible, assumptions. The first approach by White and Sully (1987) was originally developed assuming the Gardner (1958) model for the hydraulic conductivity function. The second approach developed by Haverkamp et al. (1994) and Smettem et al. (1994) does not expect any specific hydraulic functions, but requires that these functions follow a specific equation defining the infiltration constant β (equation 6 in Haverkamp et al., 1994).

Eq. (9) may also simplify and improve estimates for K_s, as λ_c is an important and often unknown parameter in many infiltration models. Four examples of methods that require λ_c to estimate K_s from steady-state infiltration data include:

i) the One-Ponding Depth (**OPD**) method by Reynolds and Elrick (1990)

$$K_s = \frac{\frac{i_s \pi r^2}{\lambda_c}\left(0.316\frac{d}{r}+0.184\right)}{r\left(\frac{H}{\lambda_c}+1\right)+\left(0.316\frac{d}{r}+0.184\right)\frac{\pi r^2}{\lambda_c}} \qquad (10)$$

ii) Method 2 by Wu et al. (1999) (**WU2**)

$$K_s = \frac{i_s}{0.9084\left(\frac{H+\lambda_c}{G^*}+1\right)} \qquad (11)$$

iii) the Steady version of the Simplified method based on a Beerkan Infiltration run (**SSBI**) by Bagarello et al. (2017)

$$K_s = \frac{i_s}{\frac{\gamma \gamma_w \lambda_c}{r}+1} \qquad (12)$$

iv) Approach 4 (**A4**) by Stewart and Abou Najm (2018b)

$$K_s = \frac{i_s}{\left(\frac{H+\lambda_c}{G^*}+1\right)} \qquad (13)$$

where d (L) is the ring insertion depth into the soil, r (L) is the ring radius, $G^* = d + r/2$, H (L) is the ponding depth of water, and γ_w is a dimensionless constant related to the shape of the wetting front (White and Sully, 1987). γ, the infiltration constant defined above, was set equal to 0.75 (Smettem et al., 1994) and γ_w was set equal to 1.818, as suggested by Reynolds and Elrick (2002).

3. Material and methods

3.1. Analytically generated data

We assessed the accuracy of the proposed calculation approach for λ_c and K_s by using the same six soils considered by Hinnell et al. (2009) and Bagarello et al. (2017): sand, loamy sand, sandy loam, loam, silt loam, silty clay loam. These soils were chosen to cover a wide range of hydraulic responses. We modelled the infiltration experiments for these synthetic soils using the infiltration model proposed by Smettem et al. (1994):

$$I(t) = I_{1D}(t) + \frac{\gamma S^2}{r_d \Delta\theta} \tag{14}$$

where I (L) is 3D cumulative infiltration and I_{1D} (L) is the 1D cumulative infiltration into an uniform, initially unsaturated soil profile, which can be modelled by the following implicit equation (Haverkamp et al., 1990):

$$\frac{2\Delta K^2}{S^2} t = \frac{1}{1-\beta}\left[\frac{2\Delta K}{S^2}\left(I_{1D}(t) - K_i t\right) - ln\left(\frac{exp\left(2\beta\frac{\Delta K}{S^2}\left(I_{1D}(t) - K_i t\right)\right) + \beta - 1}{\beta}\right)\right] \tag{15}$$

To also test the effect of the initial soil water content on parameters predictions, initial values of Se, ranging from 0.1 to 0.8 were converted to equivalent θ_i values for each soil using the relationship $Se = (\theta_i - \theta_r)/(\theta_s - \theta_r)$, with θ_r (L^3 L^{-3}) representing the residual water content. The sorptivity was then estimated as follows (Parlange, 1975):

$$S = \sqrt{\int_{h(\theta_i)}^{0} (\theta_s + \theta - 2\theta_i) K(h) dh} \tag{16}$$

The integrals in Eqs. (16) and (1) were computed using the intg function defined in Scilab (Campbell et al., 2010). The water retention curve and the hydraulic conductivity functions were calculated according to the van Genuchten–Mualem model (Mualem, 1976; van Genuchten, 1980):

$$Se = \left[\frac{1}{1 + (\alpha_{VG}|h|)^n}\right]^m \tag{17a}$$

$$m = 1 - \frac{1}{n} \tag{17b}$$

$$K(Se) = K_s Se^l\left[1 - \left(1 - Se^{1/m}\right)^m\right]^2 \tag{17c}$$

where α_{VG} (L^{-1}) is an empirical parameter related to the water pressure head, *n* is the pore size distribution index, and *l* is the pore connectivity parameter, which we assumed to be 0.5 following Mualem (1976). Hydraulic parameters for the six synthetic soils were taken from Carsel and Parrish (1988), with K_s values reported in that text used to represent the reference saturated hydraulic conductivity (**Table 2**). Default values of $\beta = 0.6$ and $\gamma = 0.75$ were assumed, as commonly suggested by many investigations (Angulo-Jaramillo et al., 2019).

To ensure steady-state conditions, each infiltration process was modelled for a period three times longer than the maximum time for which the explicit short-term expansion of Eq.(15) (Haverkamp et al., 1994) is considered valid, with t_{max} (T) calculated as follows (Lassabatere et al., 2006):

$$t_{max} = \frac{1}{4(1-B)^2}\left(\frac{S}{K_s}\right)^2 \tag{18a}$$

$$B = \frac{2-\beta}{3}\left(1 - \frac{K_i}{K_s}\right) + \frac{K_i}{K_s} \tag{18b}$$

These analytical data were used to estimate the intercept, b_s (L), and the slope, i_s (L T^{-1}), by linear regression analysis of the last three data points of the cumulative infiltration time series. Then, we defined the estimator for λ_c, $\hat{\lambda}_c$, using Eq. (9) and the estimator for K_s, $\widehat{K}_s$, via the standard predictive equations for K_s (Eqs. 10-13).

The reference macroscopic capillary length, λ_c, was calculated for each combination of soil type and initial *Se* value using Eq. (2). Relative error, *Er*, was then calculated for each estimated value for $\hat{\lambda}_c$ and $\widehat{K}_s$ compared to the corresponding reference value (i.e., λ_c and K_s) as follows:

$$Er(x) = 100 \times \frac{\hat{x}-x}{x} \tag{19}$$

where $\hat{x}$ is the estimated value and *x* is the target, i.e., the reference value λ_c (Eq. 2) or K_s (**Table 2**). According to the accuracy criterion by Reynolds (2013), the estimates were deemed accurate when they fell within the range $0.75 \leq \hat{x}/x \leq 1.25$ (i.e. $\leq$ 25% error). This stringent criterion was used because the parameters were estimated by analytically generated data, and therefore were free of the perturbations embedded in field and laboratory measurements (e.g., measurement error, random noise and natural variability).

3.2. The Beerkan infiltration database

In this investigation we also considered a large database of single ring (Beerkan) infiltration experiments carried out in four different countries, Italy, Burundi, France and Spain, during the period 2010-2017 (**Table 3**). Nearly half of the runs were carried out in Sicily, Italy (202 out of 433), and another ~1/3 of the runs (152 out of 433) were carried out in Burundi in the African Great Lakes region. The tested soils covered a range of textures, from sandy to clayey (**Figure 1**).

The Beerkan experiment is a variation of the single-ring infiltrometer technique, which consists of infiltrating water through a ring inserted shallowly (e.g., 1 cm) into the soil with a quasi-zero head of water imposed on the soil surface (Braud et al., 2005). All Beerkan experiments were carried out according to the methodology described by Lassabatere et al. (2006). First, a stainless steel ring was inserted shallowly into the soil (~1 cm). Then, water was poured on the confined soil surface in fixed volume increments (V) to establish and maintain ponding conditions. The increments, V, ranged from 17 to 800 mL depending on ring diameter (**Table 3**). The energy of the falling water was dissipated with fingers to minimize the soil disturbance owing to water pouring, as commonly suggested (e.g., Di Prima et al., 2019). For each poured volume, the time needed for the water to infiltrate was recorded. The total number of poured volumes varied depending on time needed to reach steady state, as required by the Beerkan method (Angulo-Jaramillo et al., 2019).

We then estimated the intercept, b_s (mm), and the slope, i_s (mm h^{-1}), of the regression line fitted to the cumulative infiltration time series. The final three data points were used, as those were assumed to represent steady state infiltration conditions. We estimated K_s by using Eqs. (10-13) and constraining λ_c through three different approaches:

- **Scenario 1:** determining λ_c through Eq. (9);
- **Scenario 2:** using $\lambda_c = 83$ mm, taking into account that it represents the suggested first approximation value for most field soils (Elrick and Reynolds, 1992);

- **Scenario 3:** using a soil-dependent λ_c value according to **Table 1**. Specifically, we used λ_c = 250 mm for soils with sand content < 20%, 83 mm for sand contents between 20 and 70%, and 28 mm when the soil had > 70% sand (Bagarello et al., 2017).

For the experimental dataset, the comparison of the estimator to the target is not possible. Indeed, we don't have any information on the real value of the macroscopic capillary length, given that previously developed methods to estimate λ_c have all presented some limitations, as discussed in the Introduction. Instead, we compared the estimates to representative values from the five soil capillarity categories suggested by Elrick and Reynolds (1992). Note that these categories were originally proposed to select a representative value for five soil texture-structure categories (**Table 1**) when calculating K_s by the OPD method (Angulo-Jaramillo et al., 2016). In this investigation, we also proposed range of values for each category as detailed in **Table 1**. The range values of the intermediate categories (strong, moderate and weak) were calculated as the mean of the representative values of two consecutive categories.

The same issue arises for the estimation of the saturated hydraulic conductivity. In this case, we chose to use the BEST-steady method proposed by Bagarello et al. (2014c) as a benchmark, as an independent K_s datum that can be used for assessing simplified procedures or validating newly developed methods. This method estimates K_s as follows:

$$K_{s,BEST} = \frac{C\, i_s}{A\, b_s + C} \qquad (20a)$$

$$A = \frac{\gamma}{r(\theta_s - \theta_i)} \qquad (20b)$$

Note that we also chose the Bagarello et al. (2014c) method because it requires the same experimental information as the λ_c-dependent methods considered in this investigation for estimating K_s, yet does not require an estimate of λ_c. We also avoided using laboratory measurements as benchmark, as they can induce experimental artifacts, such as soil compaction and samples biased by pores, that may limit their comparability with in-situ measurements (Haverkamp et al., 1999).

To compare K_s values estimated by Eqs. (10-13) with the reference $K_{s,BEST}$ values obtained by Eq. (20), we again used the relative error metric (Eq. 19). We also calculated paired differences for each method, i.e., $K_{s,BEST}$ - K_s and checked them for normality using the Kolmogorov-Smirnov test. For non-normally distributed data we used the Wilcoxon signed rank test to evaluate the median difference between paired observations at the 95% confidence level. All statistical analyses were carried out using the Minitab© computer program (Minitab Inc., State College, PA, USA).

4. Results

4.1. Analytical validation

4.1.1. Estimating λ_c from analytically generated data

When applied to the six synthetic soils, Eq. (2) yielded the highest λ_c values for fine-textured soils (**Table 4**). This is logical, since for fine soils the capillary contribution to water flow was higher than for coarser soils. More specifically, high λ_c values were associated to initially flat $K(h)$ relationships, i.e., when a decrease in pressure head determined a moderate pore emptying (Angulo-Jaramillo et al., 2016; Reynolds, 1994). Moreover, λ_c values decreased for all soils as *Se* increased.

When cumulative infiltration was calculated for all synthetic soils (**Table 2**) using Eqs. (14) and (15), all curves exhibited a typical concave shape as a function of time (**Figure 2**). As the process approached steady state, cumulative infiltration curves became approximately linear with time. This behaviour shows how the influence of capillarity decreases as the wetting front moves away from the source and the hydraulic gradient decreases (Xu et al., 2012). Note that the duration of the infiltration process decreased for higher values of *Se*, as steady-state conditions were attained in less time. In these cases, capillary forces only influenced infiltration during the early stage of the process.

The value of the linear regression model intercept, b_s, estimated from each curve was used in conjunction with the known θ_i and θ_s values to calculate λ_c using Eq. (9). Both b_s and i_s decreased in all soils as *Se* increased. b_s ranged from 3.1 to 35.1 mm, with larger values corresponding to the fine-textured silt loam and silty clay loam soils (**Table 4**). The slope of the linear regression model i_s had values as low as 1.7 mm h^{-1} (fine soil) and as high as 516.7 mm h^{-1} (coarse soil)

The estimated $\hat{\lambda}_c$ for the six synthetic soils ranged from 36.3 to 87.8 mm, and were classified only into weak or moderate capillary categories (Table 1), although those soils had textures which ranged from sand to silty clay loam. Relative error, $Er(\lambda_c)$, between estimated $\hat{\lambda}_c$ and reference λ_c values ranged from -7.9 to 23.3%, indicating that all λ_c values were accurate based on our stated criterion. The largest $Er(\lambda_c)$ values were obtained for the coarse-textured sandy and loamy sand soils under initial wet conditions (**Figure 3**). Indeed, neglecting K_i is expected to introduce more uncertainty on λ_c estimations for higher Se values. Nevertheless, λ_c estimates were sufficiently accurate also in these cases, with error always < 25%.

4.1.2. Estimating K_s from analytically generated data

The values of the slope, i_s, estimated from the analytically generated curves were used to calculate K_s by the four λ_c-dependent methods, i.e., OPD (Eq. 10), WU2 (Eq. 11), SSBI (Eq. 12), A4 (Eq. 13). Then, relative error, $Er(K_s)$, was calculated using Eq. (14) (**Figure 4**). $Er(K_s)$ ranged from -9.5 to 3.1% for OPD, from -5.4 to 7.4% for WU2, from 2.2 to 24.7% for SSBI, and from -14 to -2.4 % for A4. While we observe higher $|Er(\lambda_c)|$ values for initial wet conditions (**Figure 3**), for K_s, we observe similar trends between the four methods but also a consistent vertical shift of the $Er(K_s)$ values. For instance, for the SSBI method, lower errors corresponded to higher Se values. Conversely, for the A4 method, the errors always increased for increasing Se values, given that this method always underestimated K_s. We therefore argue that the discrepancies between the four methods were more relevant than the variations within a specific method due to different initial saturation degree. Nevertheless, the four methods always yielded K_s estimates close to the reference values, since $|Er(K_s)|$ values were always < 25%. Mean $|Er(K_s)|$ values were ordered as OPD < A4 < WU2 < SSBI, showing that the OPD method yielded the lower $|Er(K_s)|$ values.

4.2. Field testing

4.2.1. Estimating λ_c from the Beerkan infiltration database

Eq. (9) was also used to estimate λ_c from the field-based single ring (Beerkan) infiltration experiments. The procedure worked for nearly all Beerkan tests; however, six of the tests had infiltration rates that increased with time (i.e., the cumulative infiltration curves exhibited convex shapes). Fitting Eq. (5) to those data yielded negative value for the intercept, b_s, which led to negative values for λ_c, which is meaningless from a physical point of view. Those six cases – two at the Kinyami site, one at the Palermo – SAAF site, and three at the Crépieux-Charmy site – were excluded from subsequent analysis. The remaining 427 successful tests yielded λ_c values ranging from 1.5 to 737.7 mm (**Table 5**), thus covering the full range of soil capillarity categories suggested by Elrick and Reynolds (1992) (**Table 1**).

Across all soils, there was a consistent yet non-linear relationship between λ_c values and their corresponding intercepts b_s (**Figure 5a**). As shown by three different examples of λ_c estimation, cumulative infiltration shapes and times to steady-state conditions varied widely between soils with moderate (**Figure 5b**), strong (**Figure 5c**), and negligible capillarity (**Figure 5d**). In the first case (**Figure 5b**), cumulative infiltration exhibited the typical concave shape as a function of time. For this run, we estimated b_s value of 30.9 mm and a λ_c value of 49.2 mm (moderate capillarity). In the second case (**Figure 5c**), the cumulative infiltration curve exhibited a strong concave shape with a b_s value of 209.6 mm, yielding a λ_c value of 598.7 mm (strong capillarity). This behavior is typical for very fine soils, with low permeability. For this run, capillary forces predominated for almost the entire duration of the experiment. In the third case (**Figure 5d**), the cumulative infiltration curve had an almost linear shape with a b_s value of 1.0 mm, which translated to a λ_c value of 1.5 mm, i.e., lower than the considered threshold of 10 mm for negligible capillarity forces. This behaviour is typical for coarse-textured soils and occurs when the infiltration process is mainly driven by gravity. Altogether, 127 (29.7%) of the λ_c values represented strong capillarity conditions, 189 values (44.3%) represented moderate capillarity, 107 values (25.1%) represented weak capillary, and 4 values (0.9%) represented negligible capillarity.

4.2.2. Estimating K_s from the Beerkan infiltration database

The λ_c values determined through Eq. (9) were next used with four methods (i.e., OPD, WU2, SSBI, A4) to estimate K_s for the Beerkan dataset. The Wilcoxon signed rank test showed that all methods yielded K_s estimates significantly different from the BEST-steady values, and the differences between K_s and $K_{s,BEST}$ were always non-normally distributed according to the Kolmogorov-Smirnov test. However, the discrepancies between methods were always $\leq$ 25%, with the exception of the SSBI method (**Figure 6a**). The WU2 method yielded the best overall fit with the BEST-steady values, with $Er(K_s)$ values between -12.1 and 22.1%. The WU2 method yielded lower K_s estimates than the BEST-estimated values for 76% of the runs and higher K_s values for 24% of runs, and the median K_s values for the two methods differed by only a factor of 1.002. The OPD and A4 methods also performed well, though those methods tended to under-predict K_s to a greater extent than WU2, with 82% of OPD runs and 91% of A4 runs under-predicting K_s. The SSBI method, by contrast, yielded K_s values that were higher than $K_{s,BEST}$ with only a single exception. The $Er(K_s)$ values ranged from -1.0 to 32.8%, with 21% of the runs (88 out of 427) yielding higher values than the considered threshold of 25%.

Using constant (Scenario 2) or a soil-dependent (Scenario 3) λ_c values resulted in greater difference between K_s and $K_{s,BEST}$. With the constant λ_c value (Scenario 2), $Er(K_s)$ values ranged from -66.8 to 576.9% (**Figure 6b**), with 68.4% of OPD runs, 68.1% of WU2 runs, 55.7% of SSBI runs and 72.1% of A4 runs yielding higher values than the considered threshold of 25%. With the soil-dependent λ_c values (Scenario 3), $Er(K_s)$ values ranged from -82.9 to 486.5% (**Figure 6c**), with 70.5% of OPD runs, 69.3% of WU2 runs, 62.3% of SSBI runs and 74.0% of A4 runs yielding higher values than the considered threshold. These results also suggest that among the four considered methods, the SSBI was the least sensitive to the assumed λ_c value, with less runs (55.7

and 62.3% for scenario 2 and 3, respectively) yielding higher $Er(K_s)$ values than the considered threshold of 25%.

5. Discussion

In this investigation, we developed a new procedure to estimate λ_c using simple Beerkan infiltration experiments and measurements of initial and saturated soil water contents (Eq. 9). Previous investigations also suggested that the measured infiltration curve contains the necessary information to estimate λ_c (Bagarello et al., 2014d, e.g., 2013; Stewart and Abou Najm, 2018a; Wu et al., 1999). However, those methods are based on the analysis of the transient infiltration process and can be subject to considerable error, particularly due to uncertainties with the duration of the transient phase (Vandervaere et al., 2000). In contrast, the proposed method uses measurements collected during the steady-state stage of the infiltration process, where the infiltration rate (i_s) is assumed to be independent of the initial infiltration phase (Bagarello et al., 2013). Estimating λ_c using the proposed method requires linear regression analysis of cumulative infiltration versus time to determine the intercept (b_s). Because the magnitude of b_s depends on the entire cumulative infiltration curve (including the transient phase), that term is sensitive to the relative importance of capillary and gravity forces during ponded infiltration (Angulo-Jaramillo et al., 2019). Specifically, small b_s values indicate a linear infiltration curve, i.e., when gravity prevails over capillarity, which occurs primarily in coarse-textured and/or highly structured porous media. On the contrary, high intercept values indicate conditions when capillarity prevails over gravity, particularly in the transient infiltration phase, which occurs primarily in fine-textured soils. Therefore, b_s is expected to be a reliable predictor of the macroscopic capillary length, but one that necessitates collecting accurate data during the final stage of the infiltration process.

In this investigation, the proposed method (Eq. 9) was validated using both analytical and field data. The analytical verification demonstrated that Eq. (9) provided reliable λ_c estimates in nearly all conditions, including different soils and, for the same soils, under different initial soil water contents. For the field data, verification was conducted using a set of 427 Beerkan infiltration experiments carried out on different soils having a range of textural characteristics, i.e., from sandy to clayey. That analysis showed that nearly all soils (i.e., 99.1% of the experiments) yielded λ_c values falling within the realistic range $10 \leq \lambda_c \leq 1000$ mm (Reynolds and Elrick, 2002); only four cases yielded λ_c values lower than 10 mm. Further, the proposed method predicted $\hat{\lambda}_c$ values very close to the reference λ_c values, with all tests having relative errors between -23.2% and 7.9%. The consistency of Eq. (9) shows that it is a suitable method to constrain λ_c.

Many models to estimate K_s from field measurements (e.g., Eqs. 10-13), require knowledge of λ_c, which is often estimated based on general descriptions of soil textural and structural characteristics (e.g., **Table 1**). Previous research has shown that choosing an incorrect capillarity category can lead to threefold or greater error in estimated K_s (Bagarello et al., 2014d), and that K_s estimates are more sensitive to underpredictions of λ_c compared with overpredictions (Stewart and Abou Najm, 2018b). In this investigation we demonstrated that using constant or a soil-dependent λ_c value may result in considerably greater relative error when predicting K_s. Specifically, using Eq. (9) resulted in relative errors < 25% for all Beerkan tests when analyzed with three of the four methods, and < 30% when the fourth method was used. By comparison, assuming $\lambda_c = 83$ mm resulted in relative error up to 600%, and using a soil-dependent λ_c value caused relative errors of close to 500%.

Beyond its use in estimating K_s, λ_c can provide information on soil pore structure and water retention (Stewart and Abou Najm, 2018b), making it important to have a simple method for use in the field. For example, the proposed method for constraining λ_c may also facilitate the estimation of dynamic indicators, such as the flow-weighted mean pore radius and the number of hydraulically active pores per unit area previously proposed by Warrick and Broadbridge (1992) and Watson and Luxmoore (1986). The flow-weighted mean pore radius represents the size of pores that are actively conducting and it expresses the ability of a soil to transmit water (Reynolds and Elrick, 2005). These indicators, quantitatively linked to λ_c and K_s, are useful to understand the effects of land use and management on soil physical quality (Bouarafa et al., 2019; Castellini et al., 2019; Iovino et al., 2016). Therefore, accurate estimation of λ_c through Eq. (9) could also facilitate determination of dynamic indicators from infiltration experiments and improve soil quality assessment.

6. Summary and conclusions

In this investigation, we assessed a simple field method for estimating the macroscopic capillary length, λ_c, by only using a single-ring infiltration experiment of the Beerkan type and a measurement of the initial and saturated soil water contents. We validated the proposed method using both analytically generated data and a large database of 433 Beerkan infiltration experiments carried out in four countries (Italy, Burundi, France and Spain) over the period 2010-2017. The analytical validation supported our hypothesis that the intercept, b_s, is a reliable predictor of the macroscopic capillary length, while the testing carried out using the Beerkan database increased our confidence that the approach performs well under field conditions. Therefore, we conclude that the method proposed here constitutes an easy and effective solution for constraining λ_c, which at the same time can help users to better estimate K_s from field infiltration measurements. The proposed procedure may also avoid uncertainty due to an imprecise description of the transient state of infiltration, and any subjectivity caused by the selection of a representative λ_c value based solely on textural or structural characteristics.

Funding: This work was supported through the INFILTRON Project (ANR-17-CE04-0010, Package for assessing infiltration & filtration functions of urban soils in stormwater management; https://infiltron.org/) funded by the French National Research Agency (ANR), and the “Programma Operativo Nazionale (PON) Ricerca e Innovazione 2014-2020 (Linea 1 - Mobilità dei ricercatori, AIM1853149, CUP: J54I18000120001) funded by the European Regional Development Fund (ERDF) and the Italian Ministry of Education, University and Research (MIUR).

Author Contributions: SDP outlined the investigation and wrote the first draft of the manuscript. SDP, MI, VB, LL and RDS developed the theory. SDP, MAN, RAJ, FG, MP and MC planned the analytical validation and analyzed the field data. All authors contributed to discussing the results and developing the final version of the manuscript.

Conflicts of Interest: The authors declare no conflict of interest.

References

Alagna, V., Bagarello, V., Di Prima, S., Iovino, M., 2016. Determining hydraulic properties of a loam soil by alternative infiltrometer techniques. Hydrological Processes 30, 263–275. https://doi.org/10.1002/hyp.10607

Angulo-Jaramillo, R., Bagarello, V., Di Prima, S., Gosset, A., Iovino, M., Lassabatere, L., 2019. Beerkan Estimation of Soil Transfer parameters (BEST) across soils and scales. Journal of Hydrology 576, 239–261. https://doi.org/10.1016/j.jhydrol.2019.06.007

Angulo-Jaramillo, R., Bagarello, V., Iovino, M., Lassabatère, L., 2016. Infiltration Measurements for Soil Hydraulic Characterization. Springer International Publishing.

Bagarello, V., Castellini, M., Di Prima, S., Giordano, G., Iovino, M., 2013. Testing a Simplified Approach to Determine Field Saturated Soil Hydraulic Conductivity. Procedia Environmental Sciences 19, 599–608. https://doi.org/10.1016/j.proenv.2013.06.068

Bagarello, V., Castellini, M., Di Prima, S., Iovino, M., 2014a. Soil hydraulic properties determined by infiltration experiments and different heights of water pouring. Geoderma 213, 492–501. https://doi.org/10.1016/j.geoderma.2013.08.032

Bagarello, V., Di Prima, S., Giordano, G., Iovino, M., 2014b. A test of the Beerkan Estimation of Soil Transfer parameters (BEST) procedure. Geoderma 221–222, 20–27. https://doi.org/10.1016/j.geoderma.2014.01.017

Bagarello, V., Di Prima, S., Iovino, M., 2017. Estimating saturated soil hydraulic conductivity by the near steady-state phase of a Beerkan infiltration test. Geoderma 303, 70–77. https://doi.org/10.1016/j.geoderma.2017.04.030

Bagarello, V., Di Prima, S., Iovino, M., 2014c. Comparing Alternative Algorithms to Analyze the Beerkan Infiltration Experiment. Soil Science Society of America Journal 78, 724. https://doi.org/10.2136/sssaj2013.06.0231

Bagarello, V., Di Prima, S., Iovino, M., Provenzano, G., 2014d. Estimating field-saturated soil hydraulic conductivity by a simplified Beerkan infiltration experiment. Hydrological Processes 28, 1095–1103. https://doi.org/10.1002/hyp.9649

Bagarello, V., Di Prima, S., Iovino, M., Provenzano, G., Sgroi, A., 2011. Testing different approaches to characterize Burundian soils by the BEST procedure. Geoderma 162, 141–150. https://doi.org/10.1016/j.geoderma.2011.01.014

Bagarello, V., Iovino, M., Elrick, D., 2004. A Simplified Falling-Head Technique for Rapid Determination of Field-Saturated Hydraulic Conductivity. Soil Science Society of America Journal 68, 66. https://doi.org/10.2136/sssaj2004.6600

Bouarafa, S., Lassabatere, L., Lipeme-Kouyi, G., Angulo-Jaramillo, R., 2019. Hydrodynamic Characterization of Sustainable Urban Drainage Systems (SuDS) by Using Beerkan Infiltration Experiments. Water 11, 660. https://doi.org/10.3390/w11040660

Bouwer, H., 1964. Unsaturated Flow in Ground-Water Hydraulics. Journal of the Hydraulics Division 90, 121–144.

Braud, I., De Condappa, D., Soria, J.M., Haverkamp, R., Angulo-Jaramillo, R., Galle, S., Vauclin, M., 2005. Use of scaled forms of the infiltration equation for the estimation of unsaturated soil hydraulic properties (the Beerkan method). European Journal of Soil Science 56, 361–374. https://doi.org/10.1111/j.1365-2389.2004.00660.x

Campbell, S.L., Chancelier, J.-P., Nikoukhah, R., 2010. Modeling and Simulation in Scilab/Scicos with ScicosLab 4.4, 2nd ed. Springer-Verlag, New York.

Carsel, R.F., Parrish, R.S., 1988. Developing joint probability distributions of soil water retention characteristics. Water Resour. Res. 24, 755–769. https://doi.org/10.1029/WR024i005p00755

Castellini, M., Di Prima, S., Iovino, M., 2018. An assessment of the BEST procedure to estimate the soil water retention curve: A comparison with the evaporation method. Geoderma 320, 82–94. https://doi.org/10.1016/j.geoderma.2018.01.014

Castellini, M., Fornaro, F., Garofalo, P., Giglio, L., Rinaldi, M., Ventrella, D., Vitti, C., Vonella, A.V., 2019. Effects of No-Tillage and Conventional Tillage on Physical and Hydraulic Properties of Fine Textured Soils under Winter Wheat. Water 11, 484. https://doi.org/10.3390/w11030484

Di Prima, S., Bagarello, V., Lassabatere, L., Angulo-Jaramillo, R., Bautista, I., Burguet, M., Cerdà, A., Iovino, M., Prosdocimi, M., 2017. Comparing Beerkan infiltration tests with rainfall simulation experiments for hydraulic characterization of a sandy-loam soil. Hydrological Processes 31, 3520–3532. https://doi.org/10.1002/hyp.11273

Di Prima, S., Castellini, M., Majdi R. Abou Najm, Stewart, R.D., Angulo-Jaramillo, R., Winiarski, T., Lassabatere, L., 2019. Experimental assessment of a new comprehensive model for single ring infiltration data. Journal of Hydrology 573, 937–951. https://doi.org/10.1016/j.jhydrol.2019.03.077

Di Prima, S., Concialdi, P., Lassabatere, L., Angulo-Jaramillo, R., Pirastru, M., Cerda, A., Keesstra, S., 2018a. Laboratory testing of Beerkan infiltration experiments for assessing the role of soil sealing on water infiltration. CATENA 167, 373–384. https://doi.org/10.1016/j.catena.2018.05.013

Di Prima, S., Lassabatere, L., Bagarello, V., Iovino, M., Angulo-Jaramillo, R., 2016. Testing a new automated single ring infiltrometer for Beerkan infiltration experiments. Geoderma 262, 20–34. https://doi.org/10.1016/j.geoderma.2015.08.006

Di Prima, S., Marrosu, R., Lassabatere, L., Angulo-Jaramillo, R., Pirastru, M., 2018b. In situ characterization of preferential flow by combining plot- and point-scale infiltration experiments on a hillslope. Journal of Hydrology 563, 633–642. https://doi.org/10.1016/j.jhydrol.2018.06.033

Elrick, D.E., Reynolds, W.D., 1992. Methods for analyzing constant-head well permeameter data. Soil Science Society of America Journal 56, 320. https://doi.org/10.2136/sssaj1992.03615995005600010052x

Gardner, W., 1958. Some steady-state solutions of the unsaturated moisture flow equation with application to evaporation from a water table. Soil science 85, 228–232.

Haverkamp, R., Bouraoui, F., Zammit, C., Angulo-Jaramillo, R., 1999. Soil properties and moisture movement in the unsaturated zone. Handbook of groundwater engineering.

Haverkamp, R., Parlange, J.-Y., Starr, J., Schmitz, G., Fuentes, C., 1990. Infiltration under ponded conditions: 3. A predictive equation based on physical parameters. Soil science 149, 292–300. https://doi.org/10.1097/00010694-199005000-00006

Haverkamp, R., Ross, P.J., Smettem, K.R.J., Parlange, J.Y., 1994. Three-dimensional analysis of infiltration from the disc infiltrometer: 2. Physically based infiltration equation. Water Resour. Res. 30, 2931–2935. https://doi.org/10.1029/94WR01788

Hinnell, A.C., Lazarovitch, N., Warrick, A.W., 2009. Explicit infiltration function for boreholes under constant head conditions: INFILTRATION FUNCTION FOR BOREHOLES. Water Resources Research 45, n/a-n/a. https://doi.org/10.1029/2008WR007685

Iovino, M., Castellini, M., Bagarello, V., Giordano, G., 2016. Using Static and Dynamic Indicators to Evaluate Soil Physical Quality in a Sicilian Area. Land Degrad. Develop. 27, 200–210. https://doi.org/10.1002/ldr.2263

Kutilek, M., Nielsen, D.R., 1994. Soil Hydrology. CATENA VERLAG, Reiskirchen.

Lassabatere, L., Angulo-Jaramillo, R., Soria Ugalde, J.M., Cuenca, R., Braud, I., Haverkamp, R., 2006. Beerkan estimation of soil transfer parameters through infiltration experiments—BEST. Soil Science Society of America Journal 70, 521. https://doi.org/10.2136/sssaj2005.0026

Lassabatere, L., Angulo-Jaramillo, R., Soria-Ugalde, J.M., Šimůnek, J., Haverkamp, R., 2009. Numerical evaluation of a set of analytical infiltration equations: EVALUATION INFILTRATION. Water Resources Research 45, n/a-n/a. https://doi.org/10.1029/2009WR007941

Mualem, Y., 1976. A new model for predicting the hydraulic conductivity of unsaturated porous media. Water Resour. Res 12, 513–522.

Nimmo, J.R., Schmidt, K.M., Perkins, K.S., Stock, J.D., 2009. Rapid Measurement of Field-Saturated Hydraulic Conductivity for Areal Characterization. Vadose Zone Journal 8, 142. https://doi.org/10.2136/vzj2007.0159

Parlange, J.-Y., 1975. Convergence and validity of time expansion solutions: a comparison to exact and approximate solutions. Soil Science Society of America Journal 39, 3–6.

Philip, J., 1957. The theory of infiltration: 4. Sorptivity and algebraic infiltration equations. Soil sci 84, 257–264.

Philip, J.R., 1985. Reply To “Comments on Steady Infiltration from Spherical Cavities.” Soil Science Society of America Journal 49, 788–789. https://doi.org/10.2136/sssaj1985.03615995004900030055x

Raats, P.A.C., 1976. Analytical Solutions of a Simplified Flow Equation. Transactions of the ASAE 19, 0683–0689. https://doi.org/10.13031/2013.36096

Reynolds, W., Elrick, D., 2002. 3.4.3.2.b Pressure infiltrometer. In Methods of Soil Analysis, Part 4, PhysicalMethods, Dane JH, Topp GC (eds). SSSA Book Series, No. 5. Soil Sci. Soc. Am.: Madison,Wisconsin, USA 4, 826–836.

Reynolds, W., Elrick, D., Youngs, E., 2002. 3.4.3.2 Ring or cylinder infiltrometers (vadose zone). In Methods of Soil Analysis, Part 4, PhysicalMethods, Dane JH, Topp GC (eds). SSSA Book Series, No. 5. Soil Sci. Soc. Am.: Madison,Wisconsin, USA 818–820.

Reynolds, W.D., 2013. An assessment of borehole infiltration analyses for measuring field-saturated hydraulic conductivity in the vadose zone. Engineering Geology 159, 119–130. https://doi.org/10.1016/j.enggeo.2013.02.006

Reynolds, W.D., 1994. Letter to the editor. Comment on “comparison of three methods for assessing soil hydraulic properties” by G. B. Paige and D. Hillel. Soil Science 157, 120.

Reynolds, W.D., Elrick, D.E., 2005. Chapter 6 Measurement and characterization of soil hydraulic properties. In J. Álvarez-Benedí, & R. Muñoz-Carpena (Co-Eds.), Soil-water-solute process characterization – An integrated approach. Boca Raton: CRC Press.

Reynolds, W.D., Elrick, D.E., 2002. 3.4.3.3 Constant Head Well Permeameter (Vadose Zone), in: Methods of Soil Analysis: Part 4 Physical Methods, SSSA Book Series. Soil Science Society of America, Madison, WI, pp. 844–858. https://doi.org/10.2136/sssabookser5.4.c33

Reynolds, W.D., Elrick, D.E., 1990. Ponded Infiltration From a Single Ring: I. Analysis of Steady Flow. Soil Science Society of America Journal 54, 1233. https://doi.org/10.2136/sssaj1990.03615995005400050006x

Ross, P.J., Haverkamp, R., Parlange, J.-Y., 1996. Calculating parameters for infiltration equations from soil hydraulic functions. Transport in porous media 24, 315–339.

Roulier, S., Angulo-Jaramillo, R., Bresson, L.-M., Auzet, A.-V., Gaudet, J.-P., Bariac, T., 2002. Water transfer and mobile water content measurement in a cultivated crusted soil. Soil Science 167, 201.

Smettem, K.R.J., Parlange, J.Y., Ross, P.J., Haverkamp, R., 1994. Three-dimensional analysis of infiltration from the disc infiltrometer: 1. A capillary-based theory. Water Resour. Res. 30, 2925–2929. https://doi.org/10.1029/94WR01787

Smiles, D., Knight, J., 1976. A note on the use of the Philip infiltration equation. Soil Res. 14, 103–108.

Smith, R.E., Smettem, K.R., Broadbridge, P., 2002. Infiltration theory for hydrologic applications. American Geophysical Union.

Stewart, R.D., Abou Najm, M.R., 2018a. A Comprehensive Model for Single Ring Infiltration I: Initial Water Content and Soil Hydraulic Properties. Soil Science Society of America Journal 82, 548–557. https://doi.org/10.2136/sssaj2017.09.0313

Stewart, R.D., Abou Najm, M.R., 2018b. A Comprehensive Model for Single Ring Infiltration II: Estimating Field-Saturated Hydraulic Conductivity. Soil Science Society of America Journal 82, 558–567. https://doi.org/10.2136/sssaj2017.09.0314

van Genuchten, M.T., 1980. A closed-form equation for predicting the hydraulic conductivity of unsaturated soils. Soil science society of America journal 44, 892–898.

Vandervaere, J.-P., Vauclin, M., Elrick, D.E., 2000. Transient flow from tension infiltrometers I. The two-parameter equation. Soil Science Society of America Journal 64, 1263–1272.

Warrick, A.W., Broadbridge, P., 1992. Sorptivity and macroscopic capillary length relationships. Water Resources Research 28, 427–431. https://doi.org/10.1029/91WR02599

Watson, K.W., Luxmoore, R.J., 1986. Estimating macroporosity in a forest watershed by use of a tension infiltrometer. Soil Science Society of America Journal 50, 578–582.

White, I., Sully, M.J., 1992. On the variability and use of the hydraulic conductivity alpha parameter in stochastic treatments of unsaturated flow. Water Resour. Res. 28, 209–213. https://doi.org/10.1029/91WR02198

White, I., Sully, M.J., 1987. Macroscopic and microscopic capillary length and time scales from field infiltration. Water Resour. Res. 23, 1514–1522. https://doi.org/10.1029/WR023i008p01514

Wu, L., Pan, L., Mitchell, J., Sanden, B., 1999. Measuring Saturated Hydraulic Conductivity using a Generalized Solution for Single-Ring Infiltrometers. Soil Science Society of America Journal 63, 788. https://doi.org/10.2136/sssaj1999.634788x

Xu, X., Lewis, C., Liu, W., Albertson, J.D., Kiely, G., 2012. Analysis of single-ring infiltrometer data for soil hydraulic properties estimation: Comparison of BEST and Wu methods. Agricultural Water Management 107, 34–41. https://doi.org/10.1016/j.agwat.2012.01.004

Table 1. Soil capillarity categories suggested by Elrick and Reynolds (1992), and representative λ_c (mm) values. The suggested range values are also reported.

Soil capillarity category	Representative λ_c (mm)	λ_c range values
Very strong	≥ 1000	
Strong	250	$125<\lambda_c<1000$
Moderate	83	$42\leq\lambda_c\leq125$
Weak	28	$10<\lambda_c<42$
Negligible	≤ 10	

Table 2. Soil hydraulic parameters for the five studied soils used to model the infiltration experiments, originally from Carsel and Parrish (1988).

Soil texture	Sand	Loamy Sand	Sandy Loam	Loam	Silt Loam	Silty Clay Loam
θ_r	0.045	0.057	0.065	0.078	0.067	0.089
θ_s	0.43	0.41	0.41	0.43	0.45	0.43
α_{VG} (mm^{-1})	0.0145	0.0124	0.0075	0.0036	0.002	0.001
n	2.68	2.28	1.89	1.56	1.41	1.23
K_s (mm h^{-1})	297.0	145.9	44.2	10.44	4.5	0.7
l	0.5	0.5	0.5	0.5	0.5	0.5

Table 3. Summary of the Beerkan infiltration database. Total number of Beerkan infiltration experiments (N_{tot}) = 433.

Country	Site	N	D (cm)	V (mL)	Coordinates	Reference
Burundi	Nyamutobo (Ruyigi)	77	15	150	3°27'50" S, 30°15'40" E	Bagarello et al. (2011)
Burundi	Kinyami (Ngozi)	20	15	150	2°54'30" S, 29°49'06" E	
Italy	Giampilieri	11	15	150	38°4'8" N, 15°28'26" E	Bagarello et al. (2013)
Italy	Palermo - SAAF† (Sicily)	8	30	800	38°6'25" N, 13°21'6" E	Bagarello et al. (2014b)
Italy	Caccamo (Sicily)	4	30	800	37°52'34" N, 13°38'43" E	
Italy	Corleone (Sicily)	20	30	800	37°48'35" N, 13°17'49" E	
Italy	Sparacia (Sicily)	8	30	800	37°38'11" N, 13°45'50" E	
Italy	Palermo - SAAF (Sicily)	10	8.5	64	38°6'25" N, 13°21'6" E	Bagarello et al. (2014a)
Italy	Sparacia (Sicily)	10	8.5	64	37°38'10" N, 13°45'59" E	
Italy	Palermo - Parco d'Orleans (Sicily)	10	8.5	64	38°6'26" N, 13°20'59" E	
Italy	Villabate (Sicily)	10	8.5	64	38°4'53" N, 13°25'7" E	
Italy	Palermo - SAAF (Sicily)	12	15	200	38°6'25" N, 13°21'6" E	Bagarello et al. (2014c)
Italy	Palermo - SAAF (Sicily)	4	30	800	38°6'25" N, 13°21'6" E	
Italy	Pietranera (Sicily)	4	15	200	37°32'25" N, 13°30'44" E	
Italy	Pietranera (Sicily)	4	30	800	37°32'25" N, 13°30'44" E	
Italy	Caccamo (Sicily)	4	15	200	37°52'34" N, 13°38'43" E	
Italy	Corleone (Sicily)	20	15	200	37°48'35" N, 13°17'49" E	
Italy	Sparacia (Sicily)	8	15	200	37°38'11" N, 13°45'50" E	
Burundi	Nyamutobo (Ruyigi)	75	15	150	3°27'50" S, 30°15'40" E	
Italy	Palermo - Parco d'Orleans (Sicily)	10	15	150	38°6'26" N, 13°20'59" E	Alagna et al. (2016)
Italy	Palermo - SAAF (Sicily)	10	15	150	38°6'25" N, 13°21'6" E	Di Prima et al. (2016)
Italy	Palermo - Parco d'Orleans (Sicily)	10	15	150	38°6'26" N, 13°20'59" E	
Italy	Sparacia (Sicily)	10	15	150	37°38'10" N, 13°45'59" E	
France	Crépieux-Charmy (Lyon)	9	15	150	45°47'42" N, 4°53'19" E	
Spain	Les Alcusses de Moixent (Valencia)	10	8.5	48	38°48'33"N, 0°49'3"O	Di Prima et al. (2017)
Italy	Palermo - SAAF (Sicily)	5	5	17	38°6'25" N, 13°21'6" E	Di Prima et al. (2018a)
Italy	Palermo - Parco d'Orleans (Sicily)	5	5	17	38°6'26" N, 13°20'59" E	
Italy	Sparacia (Sicily)	5	5	17	37°38'10" N, 13°45'59" E	
Italy	Baratz Lake watershed (Sardinia)	40	8	43	40°41'53" N, 8°14'4" E	Di Prima et al. (2018b)

† Department of Agricultural, Food and Forest Sciences (SAAF = Scienze Agrarie, Alimentari e Forestali).

N = Number of Beerkan infiltration experiments; D (cm) = ring diameter; V (mL) = water volume applied with each pouring.

Table 4. Summary of the soil hydraulic properties for the six synthetic soils.

Soil	*Se*	h_i (mm)	θ_i (m^3m^{-3})	*S* (mm $h^{-0.5}$) (Eq. 16)	ϕ (mm^2 h^{-1}) (Eq. 1b)	λ_c (mm) (Eq. 2)	$\hat{\lambda}_c$ (mm) (Eq. 9)	i_s (mm h^{-1})	b_s (mm)	$\hat{K}_s$ (mm h^{-1})			
										OPD (Eq. 10)	WU2 (Eq. 11)	SSBI (Eq. 12)	A4 (Eq. 13)
Sand	0.1	269.0	0.083	86.5	11308.6	38.1	37.2	516.7	15.0	304.3	319.1	341.3	289.8
	0.2	174.5	0.122	81.3	11298.6	38.0	37.0	515.3	13.2	304.2	319.0	341.0	289.7
	0.3	133.1	0.160	75.7	11268.5	37.9	36.8	513.3	11.5	303.7	318.5	340.3	289.3
	0.4	107.8	0.199	69.6	11202.4	37.7	36.7	510.6	9.8	302.4	317.2	338.8	288.1
	0.5	89.7	0.237	62.9	11076.7	37.3	36.7	506.5	8.2	299.8	314.4	335.9	285.6
	0.6	75.2	0.276	55.5	10854.0	36.5	37.1	500.4	6.6	294.9	309.2	330.7	280.9
	0.7	62.5	0.314	46.9	10467.3	35.2	38.2	491.1	5.1	286.1	299.8	321.6	272.3
	0.8	50.2	0.353	36.8	9776.1	32.9	40.5	476.0	3.6	270.3	282.7	305.4	256.8
Loamy Sand	0.1	483.8	0.092	58.2	5602.2	38.4	37.4	254.5	13.8	149.5	156.7	167.8	142.4
	0.2	276.4	0.128	54.7	5598.0	38.4	37.2	253.8	12.2	149.5	156.7	167.6	142.4
	0.3	195.6	0.163	50.9	5584.2	38.3	36.9	252.8	10.6	149.3	156.6	167.4	142.3
	0.4	150.0	0.198	46.8	5552.5	38.1	36.6	251.4	9.0	149.0	156.2	166.9	141.9
	0.5	119.2	0.233	42.3	5490.2	37.6	36.4	249.3	7.5	148.1	155.4	165.8	141.2
	0.6	95.9	0.269	37.3	5376.9	36.9	36.3	246.1	6.0	146.4	153.6	163.9	139.5
	0.7	76.5	0.304	31.5	5176.0	35.5	36.5	241.3	4.5	143.2	150.2	160.4	136.5
	0.8	58.9	0.339	24.6	4811.2	33.0	37.4	233.4	3.1	137.2	143.8	153.9	130.6
Sandy Loam	0.1	1765.2	0.100	36.0	2145.5	49.7	48.3	86.5	17.4	45.4	47.2	52.1	42.9
	0.2	799.2	0.134	33.8	2145.5	49.7	48.0	86.3	15.4	45.4	47.2	52.0	42.9
	0.3	494.2	0.169	31.5	2140.3	49.5	47.6	85.9	13.4	45.4	47.2	52.0	42.9
	0.4	344.1	0.203	29.0	2129.8	49.3	47.1	85.3	11.3	45.3	47.2	51.8	42.9
	0.5	253.1	0.238	26.2	2107.9	48.8	46.5	84.5	9.3	45.2	47.0	51.6	42.7
	0.6	190.3	0.272	23.1	2066.0	47.8	45.7	83.3	7.3	44.8	46.7	51.2	42.5
	0.7	142.4	0.307	19.5	1988.8	46.0	44.9	81.4	5.4	44.2	46.1	50.3	41.8
	0.8	102.3	0.341	15.2	1843.8	42.7	44.0	78.1	3.5	42.8	44.6	48.7	40.6
Loam	0.1	16941.8	0.113	20.9	719.7	69.2	67.6	24.3	24.9	10.7	11.0	12.6	10.0
	0.2	4883.1	0.148	19.6	719.6	69.2	67.2	24.2	22.0	10.7	11.0	12.6	10.0
	0.3	2330.8	0.184	18.3	718.8	69.1	66.6	24.1	19.1	10.7	11.0	12.6	10.0
	0.4	1354.4	0.219	16.8	716.5	68.9	65.9	23.9	16.2	10.7	11.0	12.6	10.0
	0.5	866.2	0.254	15.2	711.0	68.4	64.8	23.7	13.2	10.7	11.0	12.6	10.0
	0.6	579.6	0.289	13.4	699.3	67.2	63.2	23.3	10.3	10.7	11.0	12.5	10.0
	0.7	390.5	0.324	11.3	676.0	65.0	61.0	22.7	7.5	10.6	10.9	12.4	9.9
	0.8	252.5	0.360	8.8	629.2	60.5	57.7	21.6	4.7	10.4	10.8	12.1	9.8
Silt Loam	0.1	1.4×10^5	0.105	16.3	402.8	89.5	87.8	12.3	35.1	4.6	4.7	5.6	4.3
	0.2	25267.3	0.144	15.3	402.8	89.5	87.3	12.2	31.1	4.6	4.7	5.6	4.3
	0.3	9318.5	0.182	14.3	402.6	89.5	86.6	12.2	27.0	4.6	4.7	5.6	4.3
	0.4	4529.8	0.220	13.2	401.8	89.3	85.7	12.1	22.9	4.6	4.7	5.6	4.3
	0.5	2531.6	0.258	11.9	399.6	88.8	84.4	12.0	18.8	4.6	4.7	5.6	4.3
	0.6	1519.5	0.297	10.5	394.4	87.6	82.4	11.8	14.7	4.6	4.7	5.6	4.3
	0.7	933.0	0.335	8.9	383.2	85.2	79.3	11.5	10.6	4.6	4.7	5.5	4.3
	0.8	553.5	0.373	7.0	359.1	79.8	74.2	10.9	6.6	4.6	4.7	5.4	4.3
Silty Clay Loam	0.1	2.2×10^7	0.123	6.0	60.0	85.7	84.9	1.9	30.3	0.7	0.7	0.9	0.7
	0.2	1.1×10^6	0.157	5.6	60.0	85.7	84.5	1.9	26.8	0.7	0.7	0.9	0.7
	0.3	$1.9E\times10^5$	0.191	5.2	60.0	85.7	84.1	1.9	23.3	0.7	0.7	0.9	0.7
	0.4	53399.3	0.225	4.8	60.0	85.7	83.4	1.9	19.8	0.7	0.7	0.9	0.7
	0.5	19954.8	0.259	4.4	59.9	85.5	82.5	1.8	16.3	0.7	0.7	0.9	0.7
	0.6	8725.5	0.294	3.9	59.5	85.0	81.0	1.8	12.8	0.7	0.7	0.9	0.7
	0.7	4137.5	0.328	3.3	58.5	83.6	78.5	1.8	9.3	0.7	0.7	0.9	0.7
	0.8	1966.9	0.362	2.6	55.9	79.9	73.6	1.7	5.8	0.7	0.7	0.9	0.7

Table 5. Summary of the soil hydraulic properties estimated from the Beerkan database.

Statistic	λ_c	K_s (mm h^{-1})				
	(mm)	BEST-steady	OPD	WU2	SSBI	A4
	(Eq. 9)	(Eq. 20)	(Eq. 10)	(Eq. 11)	(Eq. 12)	(Eq. 13)
N	427	427	427	427	427	427
min	1.5	1.3	1.4	1.4	1.6	1.2
max	737.7	3550.9	3294.1	3493.8	3758.7	3173.7
mean	112.6	270.7	258.5	269.3	305.2	244.6
median	68.0	156.8	153.3	156.4	182.4	142.0
CV	101.3	142.0	140.1	141.3	137.6	141.3

Figure 1. Textural classification of the soils included in the Beerkan infiltration database.

Figure 2. Cumulative infiltration curves for different soils and initial effective saturation degrees, *Se*. The curves were generated analytically using Eqs. (14) and (15) and the parameters listed in **Table 2**. The labels in ordinate and abscissa report respectively the total infiltrated water and the duration of the infiltration process. Note that the duration was fixed at three times the maximum time (t_{max}) for which the explicit transient infiltration model proposed by Haverkamp et al. (19994) is valid.

Figure 3. Relative error, $Er(\lambda_c)$, of the estimated macroscopic capillary length compared to reference values for six synthetic soils listed in **Table 2**.

Figure 4. Relative error of the estimated values for saturated soil hydraulic conductivity, $Er(K_s)$, for six synthetic soils that were analyzed using four different methods. OPD = one-ponding depth (Eq. 10); WU2 = Method 2 (Eq. 11); SSBI = Steady version of the Simplified method based on a Beerkan Infiltration run (Eq. 12); A4 = Approach 4 (Eq. 13).

Figure 5. **(a)** Comparison between the estimated macroscopic capillary length, λ_c, and the intercept, b_s, of the regression line between cumulative infiltration and time under steady-state conditions. The soil capillarity categories are indicated by dashed horizontal lines. Also shown are examples of λ_c estimation for **(b)** moderate, **(c)** strong, and **(d)** negligible capillarity conditions.

Figure 6. Cumulative empirical frequency distribution of relative error in estimated saturated hydraulic conductivity, $Er(K_s)$, when 427 experiments in the Beerkan database were analyzed with the four considered methods (i.e., OPD, WU2, SSBI, A4) and λ_c was constrained **(a)** using Eq. (9), **(b)** assuming λ_c = 83 mm, **(c)** using a soil-dependent λ_c value. OPD = one-ponding depth (Eq. 10); WU2 = Method 2 (Eq. 11); SSBI = Steady version of the Simplified method based on a Beerkan Infiltration run (Eq. 12); A4 = Approach 4 (Eq. 13).

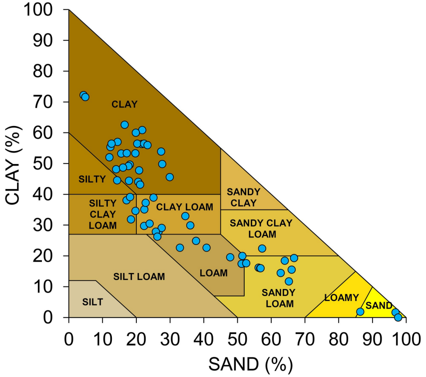
CLAY (%)
SAND (%)
CLAY
SILTY
SILTY CLAY LOAM
CLAY LOAM
SANDY CLAY
SANDY CLAY LOAM
SILT LOAM
LOAM
SANDY LOAM
LOAMY
SAND
SILT
0
10
20
30
40
50
60
70
80
90
100


Cumulative infiltration (mm)
Sand
130
115
100
86
73
60
49
38
decreasing Se values
0.07
0.09
0.11
0.13
0.15
0.17
0.20
0.22
Loamy Sand
121
106
92
78
65
53
41
30
0.12
0.15
0.19
0.23
0.28
0.32
0.37
0.42
Sandy Loam
169
149
129
109
89
70
52
35
0.40
0.57
0.75
0.94
1.14
1.34
1.55
1.75
Se
0.1
0.2
0.3
0.4
0.5
0.6
0.7
0.8
Cumulative infiltration (mm)
Loam
282
249
215
181
147
114
81
51
2.1
3.3
4.4
5.7
6.9
8.1
9.4
10.6
Time (h)
Silt Loam
461
406
351
296
241
186
131
79
6.7
10.5
14.5
18.5
22.6
26.6
30.6
34.7
Time (h)
Silty Clay Loam
389
344
298
252
207
161
115
69
37.1
59.2
81.4
103.6
125.7
147.7
169.8
191.8
Time (h)

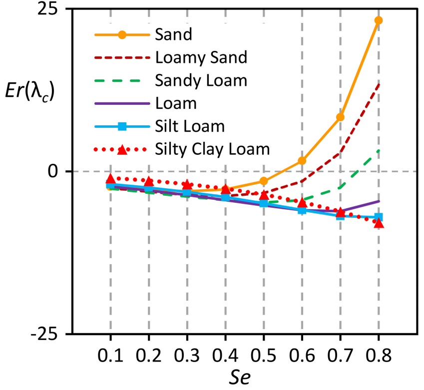
25
0
-25
$Er(\lambda_c)$
Sand
Loamy Sand
Sandy Loam
Loam
Silt Loam
Silty Clay Loam
0.1
0.2
0.3
0.4
0.5
0.6
0.7
0.8
Se

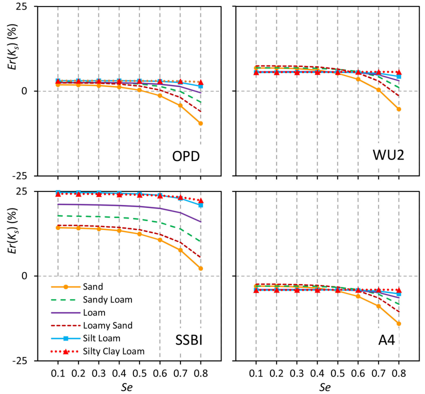
25
Er(K_s) (%)
0
-25
OPD
WU2
25
Er(K_s) (%)
0
-25
Sand
Sandy Loam
Loam
Loamy Sand
Silt Loam
Silty Clay Loam
SSBI
A4
0.1
0.2
0.3
0.4
0.5
0.6
0.7
0.8
Se
0.1
0.2
0.3
0.4
0.5
0.6
0.7
0.8
Se

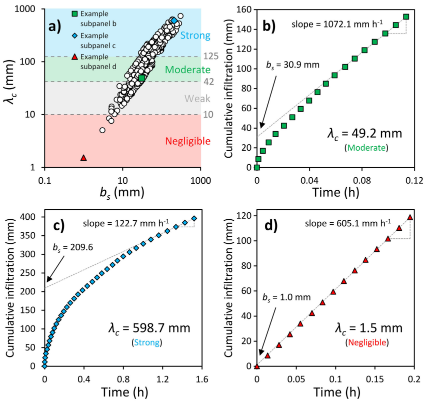
a)
λ_c (mm)
b_s (mm)
1000
100
10
1
0.1
10
1000
🟩 Example subpanel b
◆ Example subpanel c
▲ Example subpanel d
Strong
Moderate
Weak
Negligible
125
42
10
b)
slope = 1072.1 mm h-1
b_s = 30.9 mm
λ_c = 49.2 mm
(Moderate)
Cumulative infiltration (mm)
Time (h)
0
20
40
60
80
100
120
140
160
0
0.04
0.08
0.12
c)
slope = 122.7 mm h-1
b_s = 209.6
λ_c = 598.7 mm
(Strong)
Cumulative infiltration (mm)
Time (h)
0
50
100
150
200
250
300
350
400
0
0.4
0.8
1.2
1.6
d)
slope = 605.1 mm h-1
b_s = 1.0 mm
λ_c = 1.5 mm
(Negligible)
Cumulative infiltration (mm)
Time (h)
0
20
40
60
80
100
120
0
0.05
0.1
0.15
0.2

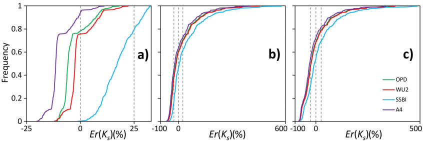
Frequency
1
0.8
0.6
0.4
0.2
0
-25
0
25
$Er(K_s)(\%)$
a)
-100
0
600
$Er(K_s)(\%)$
b)
-100
0
500
$Er(K_s)(\%)$
c)
OPD
WU2
SSBI
A4